Electrical conductivity of dense Al, Ti, Fe, Ni, Cu, Mo, Ta, and W plasmas

A. W. DeSilva
Institute for Research in Electronics and Applied Physics, University of Maryland, College Park, Maryland 20742, USA

G. B. Vunni
US Army Research Laboratory, Aberdeen Proving Ground, Maryland 20005, USA

(Received 26 October 2010; revised manuscript received 11 January 2011; published 18 March 2011)

We report measurements of electrical conductivity of eight metals in the plasma state at densities ranging from 0.002 to 0.5 times solid density, and with internal energy from 2 to 30 kJ/gm. Data are presented as functions of internal energy and specific volume. Conductivity is observed to fall as the plasma expands for fixed internal energy, and for all but tantalum and titanium shows a minimum at approximately 0.01 times solid density, followed by an increase as the density decreases further.

DOI: 10.1103/PhysRevE.83.037402 PACS number(s): 52.25.Fi, 51.50.+v, 52.27.Gr, 52.80.Qj

I. INTRODUCTION

We report here measurements of electrical conductivity made in the dense plasmas formed from elemental metal wires heated rapidly in a water bath by the electric current from discharge of a charged capacitor. Electrical conductivity measurements previously reported by the author and co-workers [1–5] required the use of tabulated equations of state from the SESAME library [6] in the analysis. In the present work, the use of such tables is avoided. Three thermodynamic variables, pressure, density, and internal energy, are measured as a function of time for each shot, and the conductivity is presented as a function of internal energy and specific volume.

II. MEASUREMENT TECHNIQUE

The experimental measurement technique is that described in Ref. [7]. Briefly, a wire sample of diameter 0.125 mm and 16.5 mm long is stretched between electrodes in the center of a water-filled chamber. A spark gap switch is closed to discharge a charged 1.88-μF capacitor into the wire, which rapidly vaporizes and enters the plasma state. The plasma column expands rapidly, and its diameter is measured from images recorded by a streak camera. Figure 1 shows an example of such a streak image. The primary observations are the voltage between the electrodes at the ends of the column, the current through the column, recorded at 4 ns intervals, and the streak camera images. Utilizing the analysis technique described in Ref. [7], we generate for each shot a table of density, internal energy, and pressure at those same intervals. Pressure is deduced from a hydrodynamic model of the water surrounding the plasma column, for which the measured column diameter is the input. For each shot, one may pick out data for plotting at specific values of internal energy.

The five plots (a)–(e) in Fig. 2 show the result of this analysis for a single shot, a discharge in a 0.125-mm-diam copper wire with an external series resistance of 2 Ω ,and a charge voltage of 15 kV on the capacitor. When the circuit is switched on, the current rises rapidly, but as the wire vaporizes, its resistance increases greatly, causing the current to drop precipitously, with simultaneous rise to a peak of the voltage along the column. The pressure spikes up steeply as expansion begins, but drops more slowly as expansion continues. Conductivity drops by a factor greater than 100, and depending on the element, passes through a minimum when the plasma volume V_r has increased by a factor of ~100 ($V_r = V/V_0$, where V and V_0 are, respectively, specific volume of the plasma and that of the metal at STP). Figure 2(d) shows temperature interpolated from the SESAME database for copper, using the measured pressure and density as input, but the temperature is not used in the analysis.

III. RESULTS

Figure 3 shows the result of 46 shots on aluminum wires 125 mm in diameter and 16.5 mm in length, made under a variety of initial conditions of charge voltage and series impedance. We display the conductivity versus V_r for several values of the internal energy density. A notable feature is the minimum in conductivity near 0.01 times solid density for

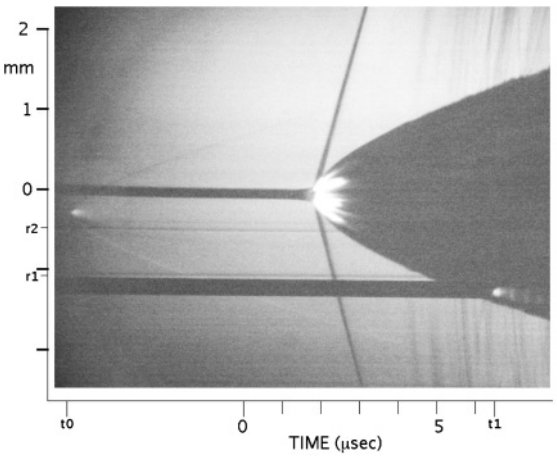

FIG. 1. Streak image of expanding plasma. The two faint lines labeled r1 and r2 provide a vertical scale. Sparks positioned at the slit, firing at times t0 and t1, make spots on the image that provide a time scale. The zero of the time scale is the time the discharge begins. The shock wave induced in the water by the sudden expansion is clearly visible, beginning at ~2 μs. Starting at ~4 μs, faint additional shock traces may be seen behind the main shock (see text). The shock wave induced in air by the spark at the slit at t0 is also visible.

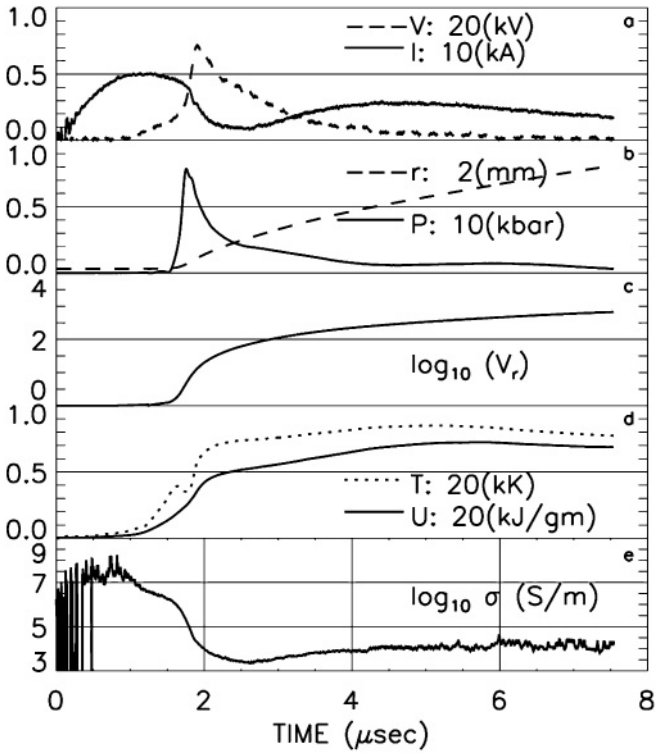

FIG. 2. Time record of a single shot, in a copper wire 0.125 mm in diameter, with a series resistance of 2 Ω and a charge voltage on the capacitor of 15 kV. (a) Current through the plasma, and the voltage between the ends, with scaling factors for each curve; (b) column radius determined by measurements on the streak image, and the pressure deduced from the hydrodynamic model; (c) specific volume, referred to that of the initial wire; (d) internal energy; (e) conductivity according to the analysis. Temperature from the SESAME database is also shown in (d).

internal energies from 12 to 24 kJ/gm. This dip in conductivity versus density disappears at the higher values of internal energy. Expansion of the plasma column that accompanies the energy input from the external circuit puts limits on our ability to measure conductivity at low energy and high volume, and for high energy and low volume. Least-squares fits to the data are also displayed. Error bars represent estimates of the effect of calibration error in current and voltage recordings, as well as digitization error, error in measurement of the column radius from the streak images, and uncertainty in locating the timing points on the streak images. Failure of some of the data points to fall within the error bars of the least-squares-fitted curves is attributed to shot-to-shot variations in the breakdown and expansion.

Figure 4 shows results of measurements on copper wires. A similar pattern of development of conductivity is seen, except that the minimum in conductivity versus volume occurs at lower energies. Conductivity of iron plasmas is displayed in Fig. 5, for which a similar pattern in conductivity versus volume is seen. Figures 6 and 7 show the data for nickel and molybdenum that follow a similar pattern as for Cu and Al. Although there is a suggestion in the 8 kJ/gm data in Fig. 7 that there might be a minimum at still lower densities, we were unable to produce conditions of low density and such low

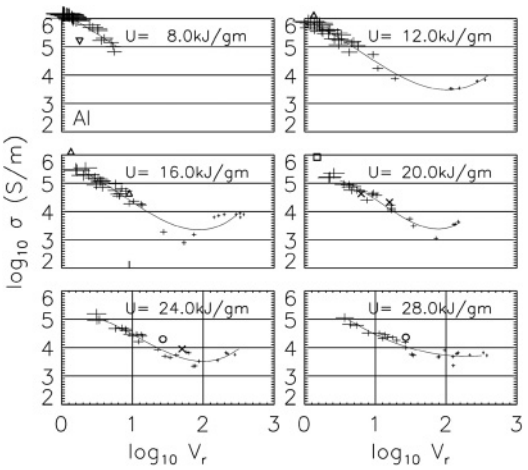

FIG. 3. Conductivity vs specific volume for aluminum plasma. The six graphs show data selected when the internal energy was within 10% of the indicated value. The point at 0.95 on the 16 kJ/g ordinate is where Redmer (Ref. [8]) places the metal-nonmetal transition. Selected data points from other work are indicated by the following symbols in some of the plots: × (Ref. [10]), □ (Ref. [11]), △ (Ref. [12]), ○ (Ref. [13]), ∇ (Ref. [14]).

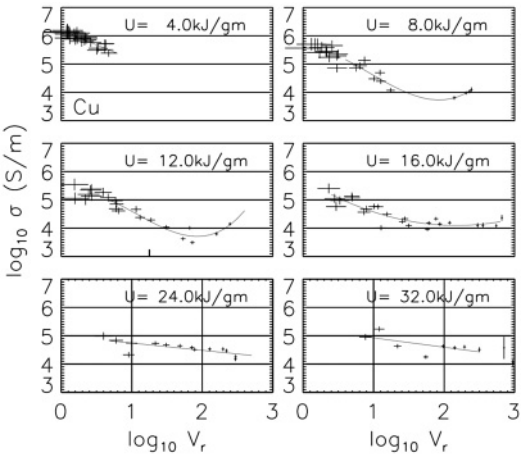

FIG. 4. Copper conductivity. The point at 1.25 on the 12 kJ/g ordinate is where Redmer (Ref. [8]) places the metal-nonmetal transition.

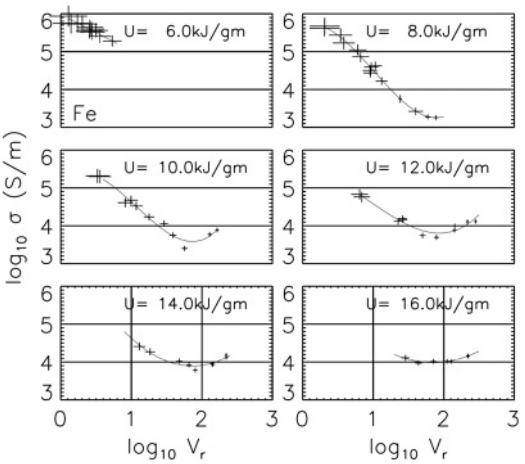

FIG. 5. Iron conductivity.

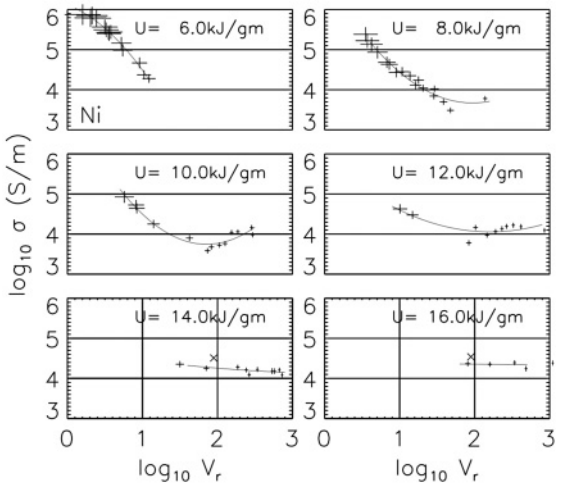

FIG. 6. Nickel conductivity. × is from Ref. [15].

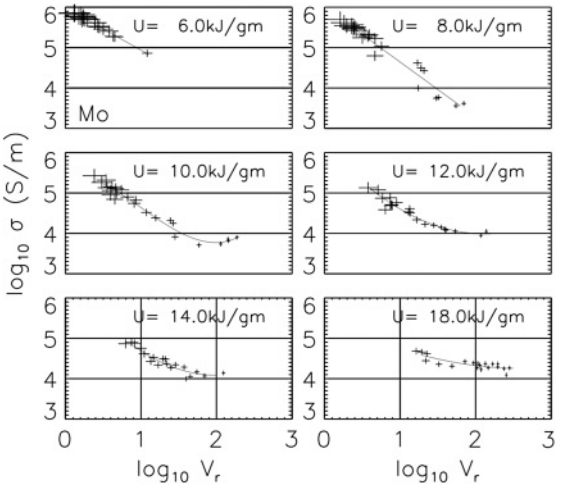

FIG. 7. Molybdenum conductivity.

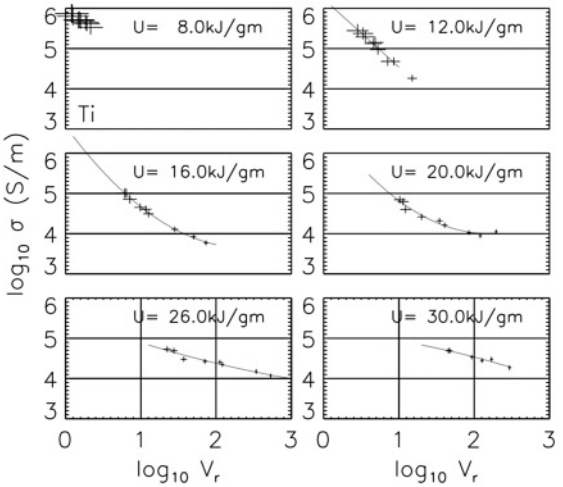

FIG. 8. Titanium conductivity. × is from Ref. [13].

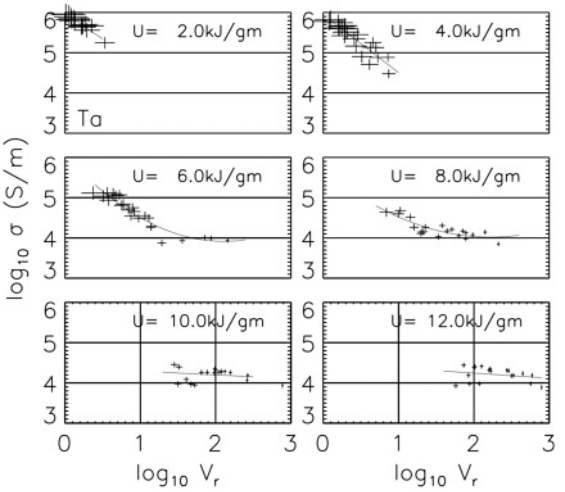

FIG. 9. Tantalum conductivity.

internal energy. In the following two plots, titanium (Fig. 8) and tantalum (Fig. 9), we found little evidence of a minimum in conductivity as the density decreased at fixed internal energy. The tungsten data (Fig. 10) again show a minimum in conductivity versus volume, but it is somewhat broader and shallower that that of the first three metals presented.

IV. DISCUSSION

A direct measurement of the plasma radiation temperature would be desirable, but, owing to the very small optical depth of the expanding plasma, observation of the absolute radiation intensity yields only a surface temperature in the boundary region at the plasma-water interface. One would expect that the temperature there would be lower that that deep within the plasma. We made such measurements, but found unrealistically low temperatures, never rising above ∼6 kK. In contrast, estimates of plasma temperature from the SESAME

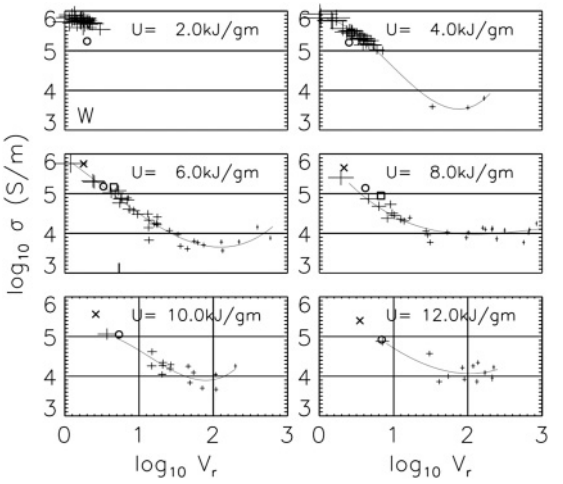

FIG. 10. Tungsten conductivity. The point at 0.73 on the 6 kJ/g ordinate is where Likalter (Ref. [9]) places the metal-nonmetal transition. Some data points from other authors' work are indicated by the following symbols: ○ (Ref. [16]), □ (Ref. [17]), × (Ref. [18]), ∇ (Ref. [19]).

database indicate typical peak temperatures closer to 20 kK through much of the plasma lifetime.

We see a steep change in conductivity for $\log(V_r)$ near unity in almost all metals investigated. This is attributed by Redmer [8] to a metal-nonmetal transition. He gives critical densities for this transition to be at approximately $V_r = 0.95$ for Al and 1.25 for Cu. Likalter [9] gives the metal-nonmetal transition point to be 3.6 g/cm^3 for tungsten, corresponding to $\log(V_r) = 0.71$. These points are indicated on the V_r axis on the left middle plot of the figures.

In the case of all but aluminum, the streak images show some structure in the shocked water outside the plasma column after 3 or 4 μs (Fig. 1). This appears to be an indication of small-scale localized instability of the plasma-water interface setting in, sending weak shocks into the surrounding water. No such indication of boundary instability is seen in the discharges in aluminum wires.

V. COMPARISON WITH OTHER WORK

We have indicated on the figures for aluminum, nickel, titanium, and tungsten some data from experiments reported by other workers. Comparison is difficult, since in most comparable work conductivity is presented with temperature T and density ρ as a parameter, rather than internal energy U and specific volume V_r as in this work. Where it is possible to find data from other reported work that intersects with ours, we have used the SESAME database to convert conductivity $\sigma(T,\rho)$ in the other work to $\sigma(U,V_r)$ for presentation in Figs. 3, 6, 8, and 10.

ACKNOWLEDGMENT

This work was supported by the US Army Research Laboratory, Aberdeen, MD.

[1] A. W. DeSilva and H.-J. Kunze, Phys. Rev. E **49**, 4448 (1994).
[2] A. W. DeSilva and J. D. Katsouros, Phys. Rev. E **57**, 5945 (1998).
[3] A. W. DeSilva and J. D. Katsouros, J. Phys. IV (France) **10**, PR5-209 (2000).
[4] A. W. DeSilva and A. D. Rakhel, Contrib. Plasma Phys. **45**, 236 (2005).
[5] A. W. DeSilva and A. D. Rakhel, Int. J. Thermophys. **26**, 1137 (2005).
[6] S. P. Lyon and J. D. Johnson, *"Sesame: the Los Alamos National Laboratory Equation of State Database,"* Report No. LA-UR-92-3407 [http://t1web.lanl.gov/doc/SESAME_3Ddatabase_1992.html].
[7] A. W. DeSilva and G. B. Vunni, Phys. Rev. E **79**, 036403 (2009).
[8] R. Redmer, Phys. Rev. E **59**, 1073 (1999).
[9] A. Likalter, Phys. Scr. **55**, 114 (1997).
[10] I. Krisch and H.-J. Kunze, Phys. Rev. E **58**, 6557 (1998).
[11] J. F. Benage, W. R. Shanahan, and M. S. Murillo, Phys. Rev. Lett. **83**, 2953 (1999).
[12] V. Recoules, J. Clerouin, P. Renaudin, P. Noiret and G. Zerah, J. Phys. A **36**, 6033 (2003).
[13] P. Renaudin, C. Blancard, G. Faussurier, and P. Noiret, Phys. Rev. Lett. **88**, 215001 (2002).
[14] A. N. Mostovych and Y. Chan, Phys. Rev. Lett. **79**, 5094 (1997).
[15] J. Clérouin, C. Starrett, G. Faussurier, C. Blancard, P. Noiret, and P. Renaudin, Phys. Rev. E **82** 046402 (2010).
[16] A. D. Rakhel, V. N. Korobenko, A. I. Savvatimski, and V. E. Fortov, Int. J. Thermophys. **25**, 1203 (2004).
[17] A. Kloss, T. Motzke, R. Grossjohann, and H. Hess, Phys. Rev. E **54**, 5851 (1996).
[18] S. Saleem, J. Haun, and H.-J. Kunze, Phys. Rev. E **64**, 056403 (2001).
[19] H. Hess, A. Kloss, A. Rekhel, and H. Schneiderbach, Int. J. Thermophys. **20**, 1279 (1999).